

# Influence of pH and pressure on the microwave-assisted hydrothermal growth of ZnIn<sub>2</sub>S<sub>4</sub>

R. BANICA<sup>a,b,\*</sup>, D. URSU<sup>a,b</sup>, P. LINUL<sup>b</sup>, T. NYARI<sup>a,b</sup>, N. VASZILCSIN<sup>a</sup>

<sup>a</sup>University Politehnica Timisoara, Piata Victoriei 2, 300006 Timisoara, Romania

<sup>b</sup>National Institute for Research and Development in Electrochemistry and Condensed Matter, 1 Plautius Andronescu Street, 300224 Timisoara, Romania

ZnIn<sub>2</sub>S<sub>4</sub> microspheres were synthesized hydrothermally in inert environment under controlled pressure. The obtained product was studied as function of pH, pressure and ballast solution type. In the 100-600 kPa range, the inert gas pressure has a large influence on the semiconductor morphology and phase purity. At higher values, the pressure influence no longer has effect. At low pressure, boiling of the solvent occurs and the obtained bubbles maintain the particles in suspension promoting growth of the spheres with low diameter. Finally, a new hypothesis on the formation of ZnIn<sub>2</sub>S<sub>4</sub> microspheres in hydrothermal environment was proposed.

(Received December 28, 2014; accepted March 19, 2015)

**Keywords:** Microwave-assisted hydrothermal, ZnIn<sub>2</sub>S<sub>4</sub>, Microspheres

## 1. Introduction

Ternary chalcogenide semiconductor ZnIn<sub>2</sub>S<sub>4</sub> was used for charge storage [1], as photoconductor material [2], and is an alternative to CdS in the construction of solar cells [3]. This compound absorbs full blue light of the solar spectrum, being an interesting material for water splitting reactions [4-6]. The values for band gap,  $E_g$ , reported in the literature for the compound ZnIn<sub>2</sub>S<sub>4</sub> are between 2.3 and 2.8 eV [4, 5, 7, 8].

This compound was synthesized by methods such as hydro-/solvothermal [4-10], spray-pyrolysis [11], chemical vapor transport [12-14]. ZnIn<sub>2</sub>S<sub>4</sub> semiconductor thin sheets were often obtained by solvothermal methods. Water [4, 5, 8], ethylene glycol [9, 10] and ethanol [15] were used as solvents. Heating the reactants was achieved, in some cases, using microwave field [4-6, 8].

So far, in the literature was not reported the influence of inert gas pressure on the properties of hydrothermally synthesized ZnIn<sub>2</sub>S<sub>4</sub> compound. In case of classical hydrothermal synthesis of microspheres, the synthesis pressure is self-generated, being determined by the vapor pressure of the solvent and the release of gases during chemical reactions [5, 6, 8]. Self-assembling of "petals" in spheres under these conditions was not extensively studied but several theories have been discussed [9]. Basically, when ZnIn<sub>2</sub>S<sub>4</sub> thin sheets form in solution, they are packed in different ways leading to the formation of nanotubes [16, 17] or microspheres [5, 15, 18]. If ZnIn<sub>2</sub>S<sub>4</sub> nanotubes can be formed from a single sheet, the microspheres are complex structures and involve self-assembly of several such sheets. Due to their porous nature, ZnIn<sub>2</sub>S<sub>4</sub> superstructures can react with high speed and can be used as self-consuming templates for the synthesis of other types of microspheres. Large pore sizes facilitate the diffusion of reactants and gaseous or highly soluble

reaction products. In liquid medium or in gaseous environment at low temperatures, where sintering does not takes place, spherical morphology can be kept. So far ZnIn<sub>2</sub>S<sub>4</sub> superstructures were not used for this purpose.

We believe that understanding the formation mechanism of ZnIn<sub>2</sub>S<sub>4</sub> spherical superstructures has great importance. In this paper the effects of pressure on microwave-assisted hydrothermally obtained ZnIn<sub>2</sub>S<sub>4</sub> are presented. Also, the effect of the pH value of precursor's solution on the morphology of the obtained product is discussed.

## 2. Experimental

### 2.1 Synthesis

A stock solution of 0.1 M ZnCl<sub>2</sub>, 0.2 M InCl<sub>3</sub> and 0.8 M (double excess) thiourea (Tu) was prepared by dissolution of p.a. purity ZnCl<sub>2</sub>, InCl<sub>3</sub>·4H<sub>2</sub>O and Tu (Sigma Aldrich) in bidistilled water. Bidistilled water and few drops of HCl solution were added to obtain 10 mL solution having different pH values and concentrations of precursors, as presented in Table 1.

These solutions were placed into Pyrex<sup>®</sup> glass vials covered with hole PTFE caps. The vials were placed in a 900 mL Teflon<sup>®</sup> jacket of SynthWAVE reactor (Milestone Inc). 300 mL ballast solution of 0.1 M Tu and pH = 2.0 (adjusted by the addition of HCl solution) was placed in the same jacket for microwave absorption.

Before starting the heating, pressure was raised using 5.0 purity compressed nitrogen (Linde Gas - Romania). The temperature was raised to 180°C with rates of 3°C/min. The reactor was maintained at this temperature for 2 hours and then it was cooled to room temperature. The product was filtered off, washed with distilled water and dried at 60°C for 1 hour in a vacuum oven.

Table 1.

Sample	Molar concentration of : Zn <sup>2+</sup> ; In <sup>3+</sup> ; Tu;	Compensating pressure (kPa)	Precursor pH value	Hydrochloric acid in ballast solution
S0_1	2·10 <sup>-2</sup> M; 4·10 <sup>-2</sup> M; 1.6·10 <sup>-1</sup> M	100	2.0	No
S0_2	5·10 <sup>-3</sup> M; 10 <sup>-2</sup> M; 4·10 <sup>-2</sup> M	100	2.6	No
S5_1	2·10 <sup>-2</sup> M; 4·10 <sup>-2</sup> M; 1.6·10 <sup>-1</sup> M	600	1.18	Yes
S5_2	2·10 <sup>-2</sup> M; 4·10 <sup>-2</sup> M; 1.6·10 <sup>-1</sup> M	600	1.6	Yes
S5_3	2·10 <sup>-2</sup> M; 4·10 <sup>-2</sup> M; 1.6·10 <sup>-1</sup> M	600	1.98	Yes
S5_4	2·10 <sup>-2</sup> M; 4·10 <sup>-2</sup> M; 1.6·10 <sup>-1</sup> M	600	2.24	Yes
S50_1	2·10 <sup>-2</sup> M; 4·10 <sup>-2</sup> M; 1.6·10 <sup>-1</sup> M	5100	2.00	Yes

## 2.2 Characterization

X-Ray Diffraction (XRD) patterns of the product were registered using an X'Pert PRO MPD PANalytical diffractometer, Ni filtered CuK $\alpha$  radiation ( $\lambda=1.541 \text{ \AA}$ ). Product morphology was investigated by Scanning Electron Microscopy (SEM) using a FEI Inspect S instrument and elemental analysis was performed by Energy Dispersive X-ray Spectroscopy (EDS). The Diffuse Reflectance Spectra (DRS) of powders were determined by a Lambda 950 (PerkinElmer) spectrometer using a 150 mm Spectralon<sup>®</sup> coated integrating sphere. Photo-luminescence (PL) spectra were obtained using FLS 980 spectrometer (Edinburgh Instruments). Excitation wavelength was 371 nm and emission spectra were detected with R928P photomultiplier. As a continuous source of radiation CW 450W Xe lamp was used.

## 3. Results and discussion

For all samples the XRD profiles (Fig. 1) are quite similar and indicate the presence of ZnIn<sub>2</sub>S<sub>4</sub> hexagonal phase, PDF 01-089-3962, as the main crystalline phase. This is in agreement with the literature for samples obtained from metal chlorides in aqueous solutions and thioacetamide [18] and thiourea in ethanol solutions, respectively [15].

Sample S0\_1, obtained at a compensating pressure of 100 kPa, is contaminated with In(OH)<sub>3</sub> (Fig. 1, sample S0\_1). Same contamination was observed in samples obtained using ballast solution with pH equal to 2 [19]. So H<sub>2</sub>S loss takes place not through a process of diffusion due to a concentration gradient of H<sub>2</sub>S between PTFE reactor and glass vials, but is due to the boiling process, as it will be seen below.

The rate of decomposition reaction of thiourea aqueous solutions is lower in acidic than in alkaline medium [20] and in the acidic range it is not strongly influenced by pH nor by the ionic strength of the solution [21].

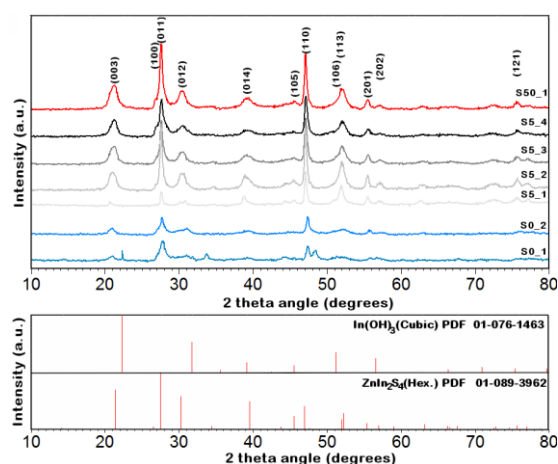
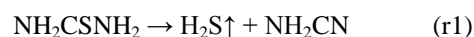
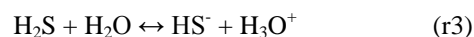


Fig. 1. XRD patterns of ZnIn<sub>2</sub>S<sub>4</sub> samples.

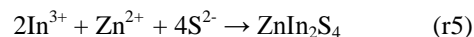
Reactions that occur in hydrothermal environment are [20]:



Hydrogen sulphide ionizes in aqueous solution according to the reactions:



Further, final product precipitates:



The pH of the ballast solution thus influences H<sub>2</sub>S concentration in the gas phase: pH decrease shifts the equilibrium reactions (r3) and (r4) toward the reduction of S<sup>2-</sup> concentration in the solution.

In samples obtained at 100 kPa nitrogen pressure, the solvent boiling occurs before reaching the temperature of 180°C. The boiling process leads to displacement of an important part of dissolved H<sub>2</sub>S from the liquid phase into the vapor phase. Accordingly, the liquid becomes deficient in sulfur ions. It was also observed that for samples

obtained without the use of compensating pressure, the volume of solvent in the glass vials shrinks by about 40-50% in the hydrothermal process. This is due to the water boiling process, so that the flow of water vapor leaving the glass vial prevents diffusion of hydrogen sulfide from the PTFE reactor chamber and the precipitation of sulphides.

Water vapor resulting from boiling condenses on the Teflon<sup>®</sup> walls of the autoclave reaching the ballast solution. At pH values between 1 and 3 indium hydroxide may be precipitated at a temperature of 180°C [22]. As for pH = 2 and the same temperature Zn(OH)<sub>2</sub> precipitation is not possible, a part of the Zn<sup>2+</sup> ions will remain in solution and In<sup>3+</sup> ions will be precipitated in the form of In(OH)<sub>3</sub>. In the presence of S<sup>2-</sup> ions, due to the small value of metal sulphides solubility product, precipitation of metal sulfides occurs before the precipitation of hydroxides.

So the solvent boiling process underlies three phenomena: *i* - reducing H<sub>2</sub>S concentration in the electrolyte solution, *ii* - preventing diffusion of H<sub>2</sub>S from the environment in the reaction medium and *iii* - keeping particles in suspension. Decreased concentration of precursors produces two other interrelated phenomena: decrease of solution supersaturation in H<sub>2</sub>S and slight increase in pH of the solution.

Under these conditions complete precipitation of metal ions with sulfide ions can occur according to reaction (r5) resulting in a pure phase ZnIn<sub>2</sub>S<sub>4</sub> (Fig. 1, S0\_2 sample). By increasing nitrogen pressure to 600 kPa and 5100 kPa respectively (at room temperature) the solvent boiling cannot occur up to 180°C. In such conditions H<sub>2</sub>S loss does not occur and the formation of pure ZnIn<sub>2</sub>S<sub>4</sub> phase can take place throughout all the studied pH range (Fig. 1, Samples S5\_1 - S5\_4 and S50\_1). XRD analysis indicates a slight trend of preferential growth of the particles in the (011) direction with increasing pressure from 600 to 5100 kPa.

### The mechanism of spheres formation

In a first step the formation of metal complexes of In<sup>3+</sup> and Zn<sup>2+</sup> with thiourea occurs, as it is noted also in [15]. This is an equilibrium reaction that releases In<sup>3+</sup> and Zn<sup>2+</sup> ions in solution. The stability of the complexes formed is low and the formation of complexes cannot prevent the formation of ZnS and In<sub>2</sub>S<sub>3</sub> at the appearance of sulfide ions in the system. Thiourea affects crystal growth rate through preferential adsorption on some crystal faces. This assumption is slightly different from that presented in [15, 23-26] but it is supported by the observation that indium and zinc sulphides can be precipitated by bubbling H<sub>2</sub>S in metal complexes with thiourea solution. The thin sheets of ZnIn<sub>2</sub>S<sub>4</sub> are probably based on In<sub>2</sub>S<sub>3</sub> clusters. Hydrothermal decomposition of the [In(Tu)<sub>3</sub>]<sup>3+</sup> complex leads to getting spheres formed from petals of In<sub>2</sub>S<sub>3</sub> [27, 28]. On the other hand, hydrothermal decomposition of [Zn(Tu)<sub>2</sub>]<sup>2+</sup> complex leads to the formation of individual ZnS nanoparticles [29] and filled spheres formed by agglomeration in different conditions of these nanoparticles [30, 31]. This means that thiourea is strongly adsorbed on some crystalline planes, rich in indium ions,

of In<sub>2</sub>S<sub>3</sub> and ZnIn<sub>2</sub>S<sub>4</sub> controlling the growth of the semiconductor sheet.

Lower pH values inhibit the formation of metal complexes with thiourea by forming coordinative bonds between non-bonding electron pairs of amine groups and hydronium ions, according to the reaction r6. Electrostatic repulsion that occurs between ligand and metal ions prevents the complexation process. Thus, supersaturation of the solution in In<sup>3+</sup> and Zn<sup>2+</sup> ions increases with decreasing of the pH.



SEM analysis indicates that pH influences the morphology of the product. At low pH values (1.18 and 1.60), the formation rate of free sheets is much larger than that of the agglomeration in spherical superstructures. In these cases large agglomerations which are quickly sedimented are formed. (Fig. 2, S5\_1 and S5\_2).

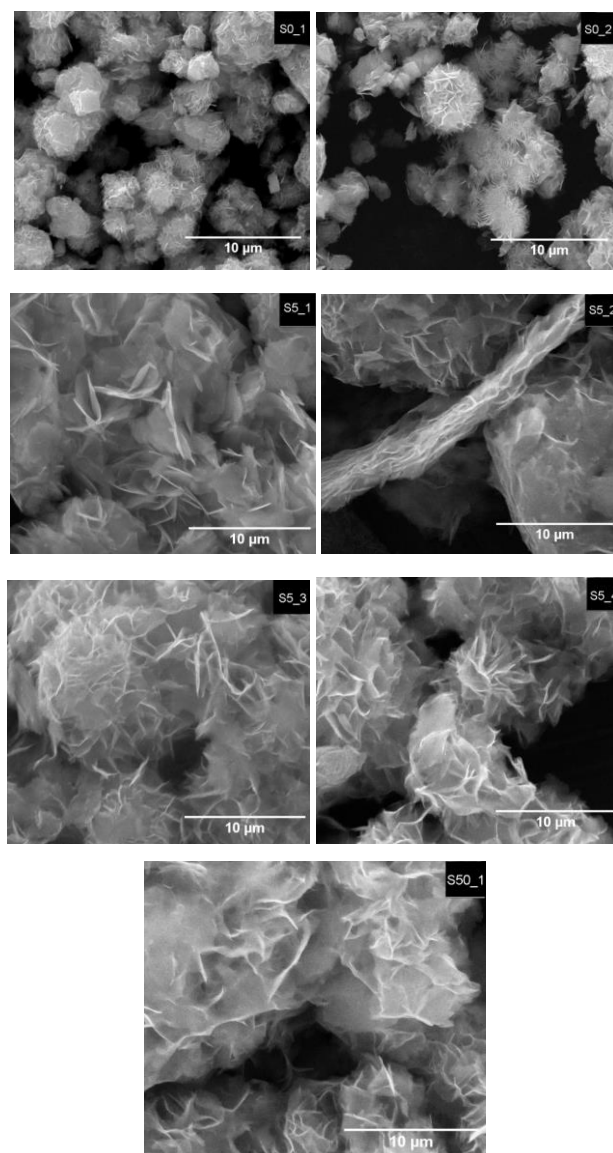


Fig. 2. SEM images of samples synthesized at different pH and pressure values.

On increasing the pH value of the precursor solution to 1.98 and 2.24,  $\text{ZnIn}_2\text{S}_4$  agglomerate spheres formation occurs, whether compensatory pressure is 600 or 5100 kPa (Fig. 2, S5\_3, S5\_4 and S50\_1). When compensating pressure drops to 100 kPa the diameter decreases regardless to precursor solution concentration, due to the boiling process that prevents agglomeration of sheets in large spheres (Fig. 2, S0\_1 and S0\_2).

TEM images for sample S5\_3 reveal the formation of  $\text{ZnIn}_2\text{S}_4$  in form of thin sheets. Since the thickness of a sheet folded in two is lower than 20 nm (Fig. 3a - inset), or the thickness of a twisted cone-shaped sheet (Fig. 3b - inset) is lower than 30 nm, it can be concluded that the thickness of a single sheet is definitely lower than 20 nm, possibly lower than 10 nm. The thickness of a single sheet of  $\text{ZnIn}_2\text{S}_4$  cannot be determined accurately in figure 3a - inset due to the radius of curvature of the sheet that makes the thickness measured in the TEM image to be greater than the real one. These sheets are on large area single crystal surfaces (Fig. 3 - c, d) that become unstable in the form of sheets in the hydrothermal environment, so their wrinkling occurs (similar to the one made on round filter paper for filtration with filter funnel) with specific surface decrease (Fig. 3a).

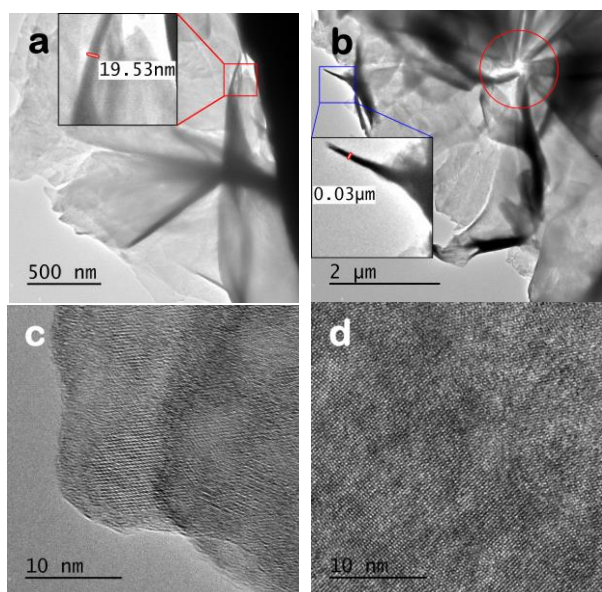


Fig. 3. TEM images of  $\text{ZnIn}_2\text{S}_4$  folded sheets for sample S5\_3 (a). "Peak to peak" assembling of folded sheets is clearly observed for same sample (b). HR-TEM images of same sample are also presented (c, d).

$\text{CO}_2$  and  $\text{H}_2\text{S}$  micro-bubbles, formed upon decomposition of thiourea in reactions r1 and r2, may be the centers producing the sheets bending. The adhesion process of sheets to the liquid-gas interface is used on large scale in the flotation process [32]. In a second stage, the wrinkled thin sheets self-assemble "peak to peak" (red circle in Fig. 3-b) forming microspheres with diameters of a few microns.

Qualitative EDS analysis revealed the presence of zinc, indium, sulfur and trace oxygen and carbon in all samples (Fig. 4). Carbon and oxygen were not quantified due to possible large errors in their determination by semi-quantitative EDS analysis.

Elemental analysis on  $\text{ZnIn}_2\text{S}_4$ , hydrothermally synthesized at pH 2.5 by Z. Chen et al, highlights also the presence of oxygen in the sample and a uniform spatial distribution of zinc, indium and sulfur [33], but no reference is made regarding the material composition or the possible substitution of  $\text{S}^{2-}$  by  $\text{O}^{2-}$  in the lattice.

The presence of oxygen is attributed to both adsorption of organic compounds [15] and semiconductor oxidation [34]. The Zn:In:S atomic ratios in the sample synthesized by using 5100 kPa compensating pressure is 1:3.05:5.4, with an atomic ratio S/(Zn + In) of 1.33, the same as for compound  $\text{ZnIn}_2\text{S}_4$ . Lowering of pH value from 2.24 to 1.18 leads to the decrease by 15.6% at. of the zinc amount in the product. Literature data indicate that for the  $\text{ZnIn}_2\text{S}_4$  compound synthesized in similar conditions (hydrothermal at pH 2.5 under microwave irradiation) global EDS analysis highlights a product slightly deficient in indium but XPS analysis highlights a compound richer in indium than the stoichiometric one [18].

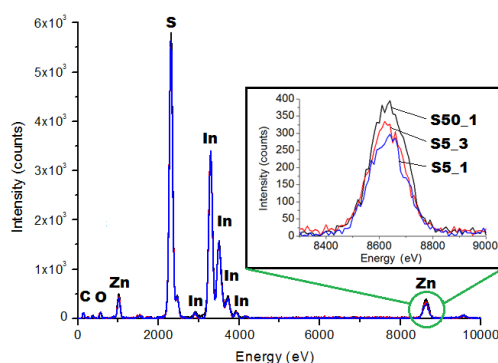


Fig. 4. EDS spectra normalized values for compounds synthesized with precursors solution at pH 1.18 - blue line, 1.98 - red-line and 600 kPa compensating pressure and pH = 2.00 and 5100 kPa compensating pressure - black line.

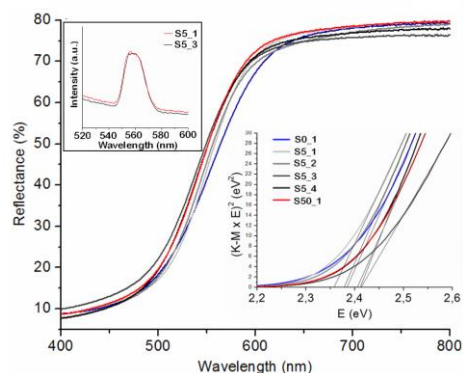


Fig. 5. DRS spectra of pure phase  $\text{ZnIn}_2\text{S}_4$  samples. Evaluation of energy band gap (inset 1) and emission spectra for two samples prepared at different pH values (inset 2).

Obtaining of non-stoichiometric compounds, rich in indium, are reported also by S. Shen et al. [34], determined by EDS and XPS analyzes of ZnIn<sub>2</sub>S<sub>4</sub> synthesized in water, methanol and ethylene glycol. However, a correlation between slightly different values of  $E_g$  and the Zn:In atomic ratio or the existence of oxygen in the bulk material cannot be done in this case [34].

Reducing the compensating pressure from 5100 kPa to 600 kPa for the same pH value of the precursor solution leads to a decrease by 16.4% at. percentage of zinc and a slight enrichment (2.3 at.%) in sulfur (Fig. 4, sample S50\_1 vs S5\_3). However, XRD spectra of these samples are very similar.

The comparative EDS and XPS data in the literature suggest that at the semiconductor-liquid interface there is an enrichment in indium of the compound which depends on pH and solvent used [34, 35]. Due to the very low thickness of ZnIn<sub>2</sub>S<sub>4</sub> sheets and, consequently, the high specific surface of the product, the number of indium ions on the surface represent a significant part of the total indium ions in the sample. This explains the EDS and XPS data which highlight the obtaining of indium-rich compounds [19, 34] by solvothermal synthesis. The existence of oxygen and carbon in the samples which are not contaminated with indium hydroxide is attributed to chemisorbed species on the surface. Some of these species can realize the charge compensation of zinc vacancies on the chalcogenide thin sheets surface.

DRS spectra (Fig. 5) shape is very similar for all samples in which pure ZnIn<sub>2</sub>S<sub>4</sub> phase is present, in accordance with XRD analysis. Band gap values were calculated using the DRS spectra. For direct band gap semiconductors,  $E_g$  could be calculated as [19, 36]:

$$\alpha h\nu = \text{const.} (h\nu - E_g)^{1/2}$$

where:  $\alpha$  is the absorption coefficient of the materials and *const.* is a proportionality constant.  $2\alpha$  is equal to Kubelka – Munk (K-M) function if the material scatters light in perfectly diffuse manner [19, 36, 37]. The value of the Kubelka – Munk function,  $f_{K-M}$ , was calculated from DSR spectrum using the equation:

$$f_{K-M} = \frac{(1-R)^2}{2R}$$

where R is the ratio between sample and standard reflectances.

The band gap energy value increases slightly with increasing pH of the precursor solution from 2.36 eV to 2.41 eV, for the samples S5\_1 and S5\_4 respectively (Fig. 5 – inset 1). This increase may be due to the slightly higher Zn:In atomic ratio with increasing pH of precursors solution. Variation of synthesis pressure does not lead to significant variations in the value of  $E_g$ . Moreover, as it was shown before [19], the increase of the heating rate does not lead to a significant variation of the  $E_g$  value of the obtained compound, but it generates an important morphology modification. PL spectra of S5\_1 and S5\_3

samples show two partially overlaid emission peaks in the 547-576 nm range (Fig. 5 – inset 2). The maximum emission at about 557 nm is due to the band-to-band transition [19], being close to 560 nm, value obtained for undoped ZnIn<sub>2</sub>S<sub>4</sub> [5].

#### 4. Conclusions

ZnIn<sub>2</sub>S<sub>4</sub> was hydrothermally synthesized in nitrogen atmosphere under microwave field at different pH values using compensating nitrogen pressure of 100, 600 and 5100 kPa and a heating rate of 3°C/min. The increase of precursors' pH influences significantly the morphology of the ZnIn<sub>2</sub>S<sub>4</sub> compound, allowing the formation of glued spheres (ZnIn<sub>2</sub>S<sub>4</sub> spheres with flower morphology) at a pressure of 600 kPa. Increasing pressure from 600 to 5100 kPa did not result in significant changes of morphology but increase of synthesis pressure leads to the slight increase of nanoparticles growth in the (011) direction. Conversely, decreasing the compensating pressure to 100 kPa allows the solvent boiling at a temperature close to 100°C and modification of precursor concentration in the reactor. Gas bubbles formed by boiling permit maintaining the ZnIn<sub>2</sub>S<sub>4</sub> particles in suspension with the formation and increase of the spheres slightly contaminated with indium hydroxide. Decreased concentration of precursors leads to the formation of pure phase ZnIn<sub>2</sub>S<sub>4</sub>. The value of semiconductor band gap is not influenced by pressure and increases slightly from 2.36 to 2.41 eV with increasing precursors' solution pH from 1.18 to 2.24, probably due to increasing Zn:In atomic ratio. Finally, based on TEM images, a new hypothesis on ZnIn<sub>2</sub>S<sub>4</sub> thin sheets self-assembly into microspheres is presented. Thus, packing of single crystalline sheets around the CO<sub>2</sub> micro-bubbles may be the first step. In a second stage, peak to peak arrangement of packed sheets occurs with porous microspheres formation.

#### Acknowledgements

This work was partially supported by the strategic grant POSDRU/159/1.5/S/137070 (2014) of the Ministry of National Education, Romania, co-financed by the European Social Fund – Investing in People, within the Sectoral Operational Programme Human Resources Development 2007-2013.

We also thank Mrs. Daniela Drasovean for her help in drafting this paper.

#### References

- [1] N. Romeo, A. Dallaturca, R. Braglia, G. Sberveglieri, *Appl. Phys. Lett.* **22**(1), 21 (1973).
- [2] T. Toyada, M. Sorazawa, H. Nakamishi, S. Endo, S. Chofu, T. Irie, *Jpn. J. Appl. Phys.*, **32**, 291 (1993).
- [3] T. T. John, M. Mathew, C. S. Kartha, K. P.

- Vijayakumar, T. Abe, Y. Kashiwaba, *Sol. Energ. Mat. Sol. C.*, **89**, 27 (2005).
- [4] Z. Lei, W. You, M. Liu, G. Zhou, T. Takata, M. Hara, K. Domen, C. Li, *Chem. Commun.*, **17**, 2142 (2003).
- [5] S. Shen, L. Zhao, L. Guo, *Int. J. Hydrogen Energ.*, **33**(17), 4501 (2008).
- [6] S. Shen, L. Zhao, X. Guan, L. Guo, *J. Phys. Chem. Solids*, **73**(1), 79 (2012).
- [7] F. Fang, L. Chen, Y - B. Chen, L-M. Wu, *J. Phys. Chem. C.*, **114**(6), 2393 (2010).
- [8] S. Shen, L. Zhao, L. Guo, *Mater. Res. Bull.*, **44**(1), 100 (2009).
- [9] X. Gou, F. Cheng, Y. Shi, L. Zhang, S. Peng, J. Chen, *J. Am. Chem. Soc.*, **128**(22), 7222 (2006)
- [10] X. Hu, J. C. Yu, J. Gong, Q. Li, *Cryst. Growth Des.* **7**(12), 2444 (2007).
- [11] M. Li, J. Su, L. Guo, *Int. J. Hydrogen Energ.*, **33**(12), 2891 (2008).
- [12] V. F. Zhitar, A. I. Machuga, E. D. Arama, **38**(6), 542 (2002).
- [13] S. Shionoya, Y. Tamoto, *J. Phys. Soc. Jpn.*, **19**(7), 1142 (1964).
- [14] N. Berand, K-J. Range, *J. Alloy. Compd.* **205**(1-2) 295 (1994).
- [15] W. Cai, Y. Zhao, J. Hu, J. Zhongand, W. Xiang, *J. Mater. Sci. Technol.*, **27**(6), 559 (2011).
- [16] X. Gou, F. Cheng, J. Shi, L. Zhang, S. Peng, J. Chen, P. Shen, *J. Am. Chem. Soc.* **128**(22), 7222 (2006).
- [17] L. Shi, P. Yin, Y. Dai, *Langmuir*, **29**(41) 12818 (2013).
- [18] Z. Chen, D. Li, G. Xiao, Y. He, Y-J. Xu, *J. Solid State Chem.* **186**, 247 (2012).
- [19] R. Banica, D. Ursu, A. V. Racu, N. Vaszilcsin, 6<sup>th</sup> International Conference on Nanomaterials, Brno, Czech R., 2014, Poster Session A, PA64.  
<http://www.nanocon.eu/files/proceedings/20/reports/3463.pdf>
- [20] Y. Chen, Y. Zheng, X. Zhang, Y. Sun, Y. Dong, *Sci China. Phys. Mech. Astron.* **48**(2) 188 (2005).
- [21] W. H. R. Shaw, D. G. Walker, *J. Am. Chem. Soc.*, **78**(22), 5769 (1956).
- [22] S. A. Wood, L. M. Samson, *Ore Geol. Rev.* **28**(1), 57 (2006).
- [23] J. Q. Hu, B. Deng, C. R. Wang, K. B. Tang, Y. T. Qian: *Mater. Chem. Phys.* **78**, 650 (2003).
- [24] J. Q. Hu, B. Deng, W. X. Zhang, K. B. Tangand, Y. T. Qian, *Int. J. Inorg. Mater.* **3**, 639 (2001).
- [25] G. Z. Shen, D. Chen, K. B. Tangand, Y. T. Qian, *J. Cryst. Growth*, **252**, 199 (2003).
- [26] J. S. Zhong, J. Hu, W. Cai, F. Yang, L. J. Liu, H. T. Liu, X. Y. Yang, X. J. Liangand, W. D. Xiang, *J. Alloy. Compd.*, **501**, L15 (2010).
- [27] S. D. Naik, T. C. Jagadale, S. K. Apte, R. S. Sonawane, M. V. Kulkarni, S. I. Patil, S. B. Ogale, B. B. Kale, *Chem. Phys. Lett.*, **452**, 301 (2008).
- [28] X. Zhu, J. Ma ,Y. Wang, J. Tao, J. Zhou, Z. Zhao, L. Xie, H. Tian, *Mater. Res. Bull.* **41**, 1584 (2006).
- [29] M. Jayalakshmi, M. Mohan Rao, *J. Power Sources* **157**, 624 (2006).
- [30] Y. Lixiong, W. Dan, H. Jianfeng ,C. Liyun, O. Haibo, W. Jianpeng, Y. Xiang, *Ceram. Int.* **41**, 3288 (2015).
- [31] J. Zhao, R. Liu, *Mater. Lett.*, **124**, 239 (2014).
- [32] M. Fan, D. Tao, R. Honaker, Z. Luo, *Mining Science and Technology* **20**, 641 (2010).
- [33] Z. Chen, J. Xu, Z. Ren, Y. He, G. Xiao, *Catal. Commun.*, **41**, 83 (2013).
- [34] S. Shen, L. Zhao, L. Guo, *J. Phys. Chem. Solids*, **69**, 2426 (2008).
- [35] Z. Chen, J. Xu, Z. Ren, Y. He, G. Xiao, *J. Solid State Chem.*, **205**, 134 (2013).
- [36] A. E. Morales, E. S. Mora, U. Pal, *Rev. Mexicana Fís.*, **S53**(5), 18 (2007).
- [37] C. Zamfirescu, I. Dincer, G.F. Naterer, R. Banica, *Chem. Eng. Sci.*, **97**, 235 (2013).

\*Corresponding author: radu.banica@yahoo.com